# CHAPTER VII - SAFETY EVALUATION OF A CONCRETE GRAVITY DAM IN SOUTH AFRICA BASED ON FRACTURE ANALYSIS

## 7.1 Introduction

Evaluation of the safety of the existing dams in South Africa is carried out on a five-year basis. Cracking in concrete gravity dams could endanger the safety of the dams and needs to be accurately simulated and analyzed. In the preceding chapters, constitutive crack models have been adopted and a bilinear crack strain-softening law has been proposed. Implementation of the models and crack constitutive relationships has been undertaken by coding a subprogram. Verification and validation of the implemented crack models by means of fracture analyses of various concrete structures, including concrete gravity dams, have been carried out.

The objective of this chapter is to use the crack analysis method developed to predict crack propagation in an existing concrete gravity dam, namely the Van Ryneveld's Pass Dam in South Africa, and to evaluate the safety of the dam under the conditions of crack development in the dam.

## 7.2 Description of the gravity dam and finite element (FE) model (with reference to Seddon, Shelly, Moore & Forbes 1998)

The Van Ryneveld's Pass Dam is a 33-m-high concrete gravity dam completed in 1925 (see Figure 7.1). The dam is situated on the Sunday's River about one km north of Graaff-Reinet. The main function of the dam is to provide storage of over 47 million $m^3$ of water for the Graaff-Reinet Municipality and for irrigation.

The dam's foundation was not grouted and no drainage system was installed. The downstream face is made of large staggered, stepped blocks.

The main features of the dam are as follows:
(RL is the "reduced" or reference level)

| | |
|---|---|
| Non-overspill crest level (walkway) | RL 790.35 m |
| Full supply level (FSL) | RL 787.60 m |
| Riverbed level | RL 757.00 m |
| Maximum height of concrete wall above riverbed | 33.35 m |
| Maximum excavation depth | 14.4 m |
| Crest thickness at NOC | 3.05 m |
| Upstream slope | vertical |
| Downstream slope (RL 772.18 m to RL 787.60 m) | 0.50: 1 (H:V) |
| Downstream slope (RL 755.40 m to RL 772.18 m) | 0.65: 1 (H:V) |
| Downstream slope (below RL 755.40 m) | 1: 1 (H:V) |

Figure 7.1 - Van Ryneveld's Pass Dam (view from downstream)

The FE model is shown in Figures 7.2 and 7.3, assuming a conservative average critical level (RL 751.30 m, 5.7 m below the riverbed level) for the concrete/rock interface over the central high part of the dam (Seddon *et al*. 1998). Plane strain elements with first-order full integration are used in the analysis.

The boundary conditions are set as follows:

All the nodes at the outer edges of the area of the foundation being considered, shown in Figure 7.2, are fixed in both horizontal and vertical translation degrees of freedom, except for the nodes on the top face on which the base of the dam is situated.

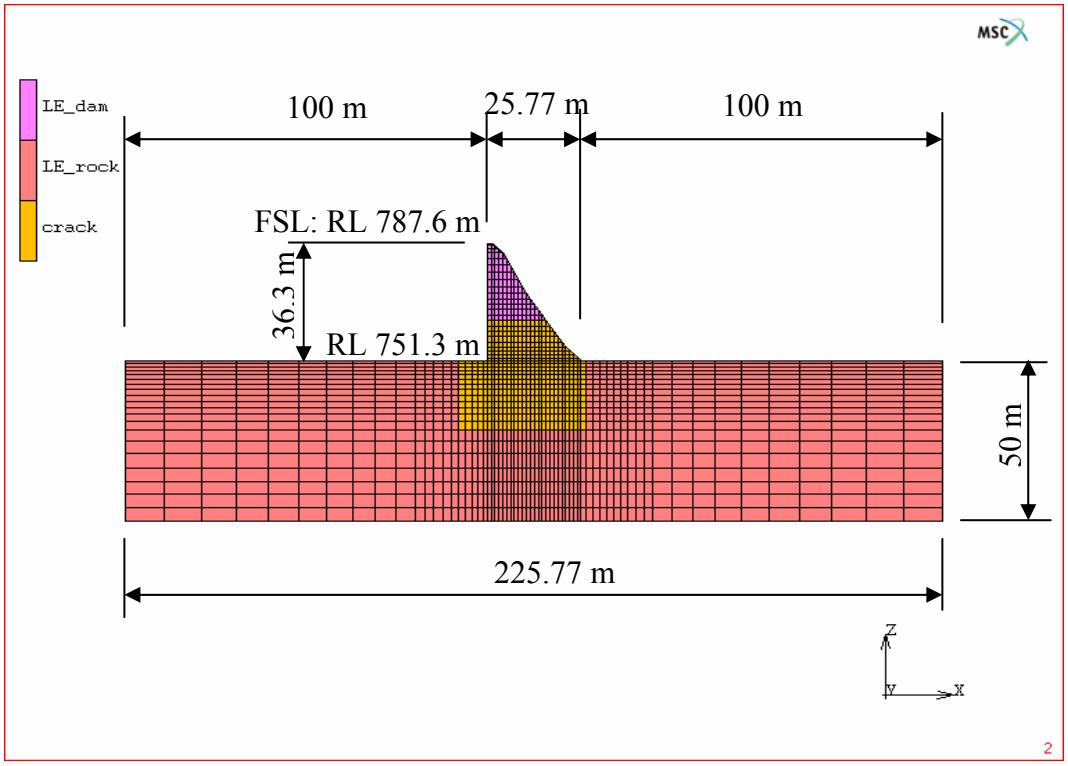


Figure 7.2 - Finite element model of Van Ryneveld's Pass Dam

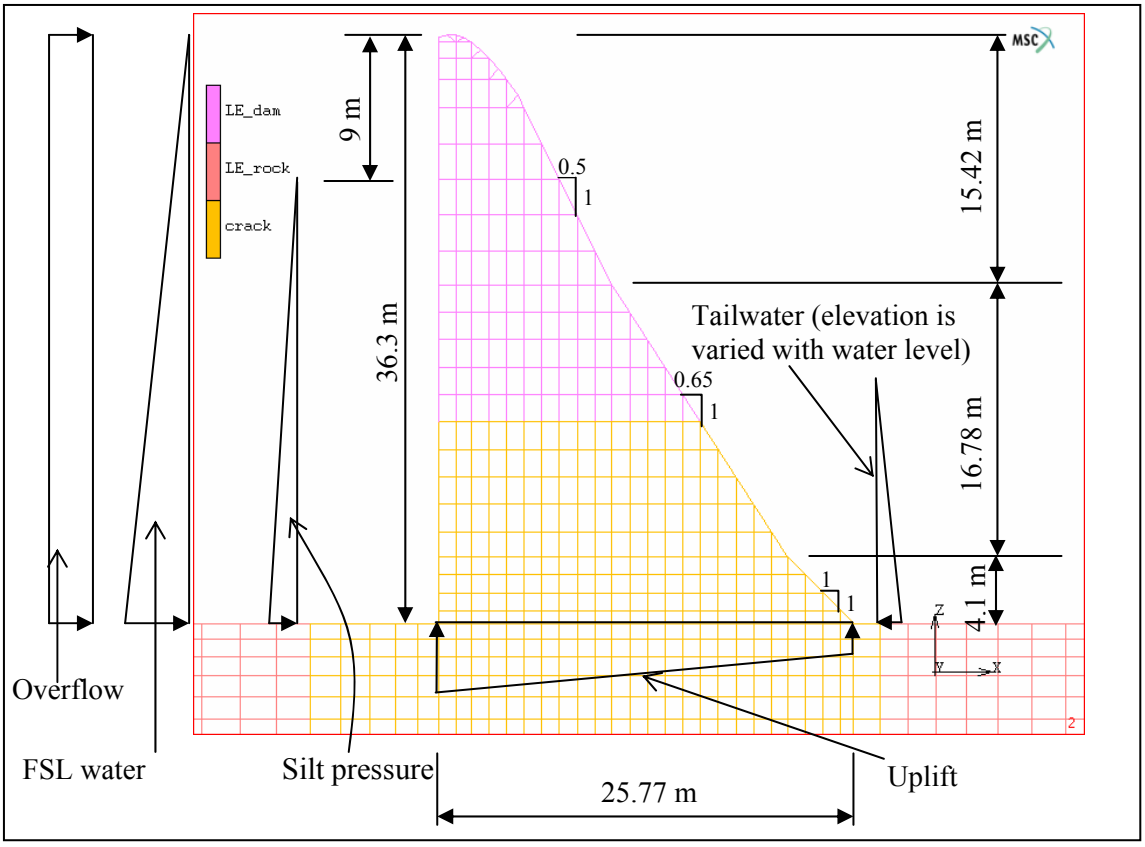


Figure 7.3 - Finite element model of Van Ryneveld's Pass Dam (close-up for dam wall) and hydrostatic and sediment loadings applied

## 7.3 Material properties and constitutive fracture parameters

The concrete used in the dam was tested from drilled cores and was fully reported by Van der Spuy (1992). The material properties of the concrete are given in Table 7.1, with reference to Van der Spuy (1992) and Seddon *et al*. (1998).

The rock foundation is reported to be sound dolerite bedrock. Schall (1988) conducted a visual inspection and laboratory tests on samples obtained by drilling through the dam's concrete wall and its rock foundation by means of five vertical holes. The tests on the rock samples showed that the rock is dolerite of excellent quality. Blake (1975) indicated that the uniaxial tensile strength of intact dolerite type of rock materials could be as high as 30 MPa. The intact shear strength of the dolerite varied in a range of 37.6 MPa to 63.3 MPa (Seddon *et al*. 1998). It is therefore reasonable to assume that the tensile strength of the fractured dolerite at the dam site to be 2.5 MPa.

The cohesion and frictional angle of the rock are matters of uncertainty because no laboratory test results are available. It is general practice for dam stability analysis in South Africa to assume that the tangent of the angle of internal friction of rock, $\tan\varphi$, is 0.8. The angle of internal friction of rock tested by the United States Bureau of Reclamation revealed that most rock samples have an angle of internal friction $\varphi \geq 45^0$ (Thomas 1976:170-171). Blake (1975:9-4–9-5) indicated $\tan\varphi$ = 1.1 for dolerite-type rock. In the present study, the angle of internal friction $\varphi$ adopted is 39°. The cohesion of the rock is assumed to be 1 MPa to 10 MPa. Non-linear plasticity analyses have been carried out based on this value range of cohesion for dolerite rock. The material properties of rock are also presented in Table 7.1.

TABLE 7.1 - Material properties of concrete and rock

| **Concrete wall** | | **Rock foundation** | |
|---|---|---|---|
| Young's modulus $E$ (MPa) | 28 000 | Young's modulus $E$ (MPa) | 30 000 |
| Poisson's ratio $v$ | 0.2 | Poisson's ratio $v$ | 0.22 |
| Tensile strength $f_t$ (MPa) | 1.5 | Tensile strength $f_t$ (MPa) | 2.5 |
| Mass density (kg/m$^3$) | 2 455 | Mass density (kg/m$^3$) | 0 |
| Cohesion (MPa) | 2.41 | Cohesion (MPa) | 1 ~ 10 |
| Frictional angle $\varphi$ | 55° | Frictional angle $\varphi$ | 39° |
| Coefficient of thermal expansion | 1.0E$^{-5}$/°C | | |

The constitutive fracture parameters of concrete and rock in the dam are also a matter of uncertainty. A sensitivity study on the fracture parameters is needed as part of a comprehensive fracture analysis of the dam for crack behaviour and safety evaluation.

## 7.4 Bilinear strain-softening shape parameters

As stated previously, concrete strain softening has been presented in the form of linear, bilinear and non-linear curve diagrams. A bilinear softening strategy provides a good approximation of the behaviour of the concrete material and has been accepted as a reasonable approximation of the softening curve for concrete. In the bilinear softening diagram, the first branch is steeper and represents large-scale debonding (fracture of

aggregates) and the second branch represents the frictional pull-out of aggregates which characterizes the behaviour of larger cracks (ICOLD report 2001).

The bilinear softening laws have been used in past investigations for the numerical analysis of concrete fracturing. High discrepancies in the values adopted for the shape parameters $\alpha_1$ and $\alpha_2$ have been reported since there is no agreement about the precise position of the kink point of concrete material. The kink position is also influenced by the type of concrete and the fracture energy $G_f$, etc.

The bilinear softening shape parameters $\alpha_1$ = 1/3 and $\alpha_2$ = 1/7 were selected by Li & Zimmerman (1998), Barpi & Valente (2001) and Yang & Proverbs (2003) in their analyses of fracturing in concrete structures such as a three-point bending beam, a dam model and a four-point shear beam.

The crack stress–crack opening relationships (see Figure 7.4) used in the above analyses had to be transformed into crack stress–strain softening laws (see Figure 7.5) for the present study. If constant strain is assumed in the crack blunt width, then the shape of the crack stress–crack opening can be viewed as the same as that of the crack stress–strain relationship. The following formula (equation 7.1) was derived for calculating $\alpha_2$ from the given values of $\alpha_1$, $W_1$ and $W_2$:

$$\alpha_2 = \frac{\alpha_1}{1-\alpha_1}\frac{W_1}{W_2 - W_1} = \frac{\alpha_1}{1-\alpha_1}\frac{\frac{W_1}{W_2}}{1-\frac{W_1}{W_2}} \qquad (7.1)$$

Shi *et al*. (2001) adopted a bilinear softening diagram in the analysis of a concrete tunnel. The bilinear softening shape parameters $\alpha_1$= 1/4 and $\alpha_2$= 1/17 were used, which are transformed by the formula in equation 7.1, from the original crack stress–crack opening relationship adopted in the analysis.

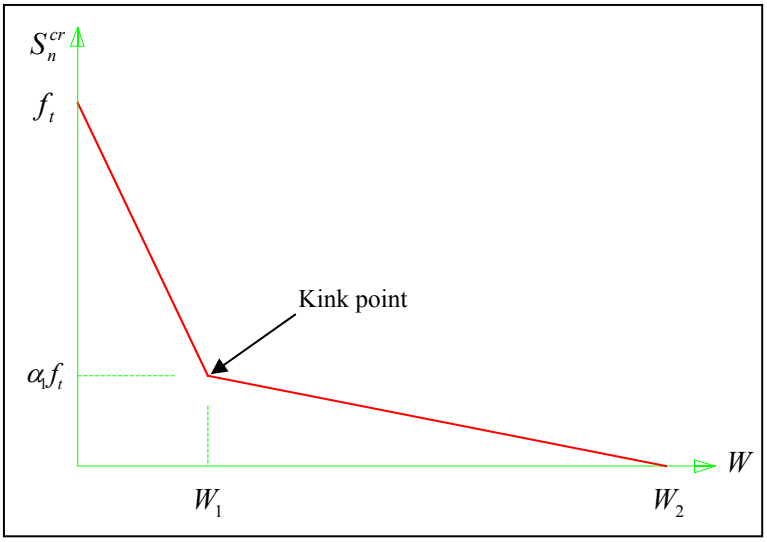


Figure 7.4 - Bilinear strain softening (tensile stress vs. crack opening displacement)

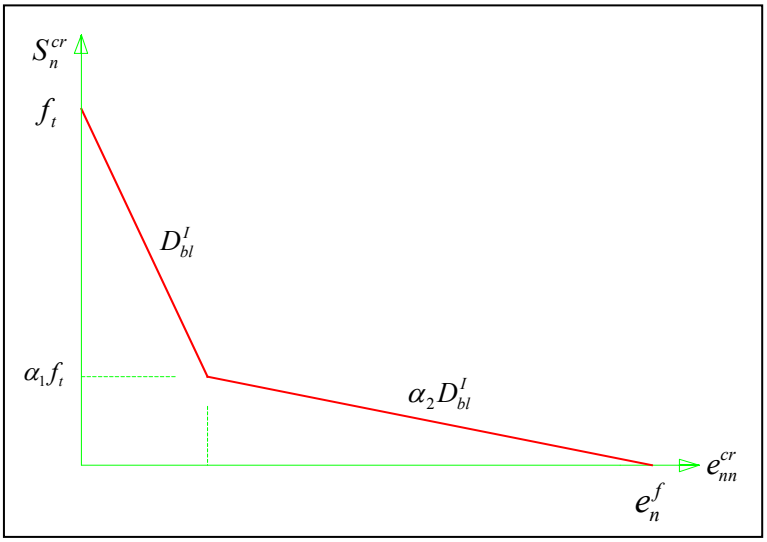


Figure 7.5 - Bilinear strain softening (tensile stress vs. local crack strain)

Gálvez *et al*. (2002) also adopted a bilinear strain-softening law in the analysis of cracking in concrete, but did not indicate the values for the bilinear softening shape parameters $\alpha_1$ and $\alpha_2$ in their paper.

Further, Hanson & Ingraffea (2003) adopted bilinear strain softening in the analysis of concrete fracturing. They undertook a comparative study on different combinations of the bilinear softening shape parameters $\alpha_1$ and $\alpha_2$. The range for $\alpha_1$ was chosen as 0.1 ~ 0.5 and $\alpha_2$ was selected from a very low value (1/171) to 1.0.

Bilinear strain softening has also been used in past investigations into the fracturing of concrete dams. Various researchers have proposed different values for the bilinear softening shape parameters $\alpha_1$ and $\alpha_2$. Petersson (1981) proposed the bilinear softening shape parameters $\alpha_1 = 0.3$ and $\alpha_2 = 0.107$ and Wittmann *et al*. (1988) proposed the bilinear softening shape parameters $\alpha_1 = 0.25$ and $\alpha_2 = 1/17$.

Feltrin, Wepf & Bachmann (1990) adopted a bilinear softening law in the seismic cracking analysis of concrete gravity dams, but gave no indication of the values of the bilinear softening shape parameters $\alpha_1$ and $\alpha_2$ used in their analysis.

Brühwiler & Wittmann (1990) conducted a series of wedge-splitting tests on the drilled cores from a concrete dam and presented bilinear strain-softening diagrams from the tests. According to the ICOLD report (2001) on the physical properties of hardened conventional concrete in dams, Brühwiler & Wittmann (1990) gave the bilinear softening shape parameters $\alpha_1 = 0.4$ and $\alpha_2 = 0.243$ for dam concrete.

Shi *et al*. (2003) also adopted a bilinear softening diagram in the analyses of concrete gravity dams. The bilinear softening shape parameters $\alpha_1 = 1/4$ and $\alpha_2 = 1/17$ were used, which are transformed by the formula in equation 7.1, from the original crack stress–crack opening relationship adopted in the analyses.

Espandar & Lotfi (2003) adopted bilinear softening diagram in the FE fracture analysis of a concrete arch dam. The bilinear softening shape parameters $\alpha_1 = 0.01$ and $\alpha_2 = 0.0001$ had been used in the analysis. Thus the bilinear softening is basically in the linear format. The very low value for $\alpha_2$ was adopted mainly for avoiding zero stiffness in the crack normal direction.

Based on the past numerical and experimental investigations into the bilinear softening crack analysis of dam concrete, a good range for the bilinear softening shape parameters would be $\alpha_1 = 0.25 \sim 0.4$ and $\alpha_2 = 0.05 \sim 0.3$ to approximate dam concrete softening behaviour. A sensitivity study on the ranges of $\alpha_1$ and $\alpha_2$ should be carried out for analyzing the cracking behaviour of concrete in dams.

## 7.5 Fracture analysis and evaluation of the dam safety

A crack analysis is carried out, studying the sensitivity of the fracture parameters and comparing the results with the linear elastic and non-linear Mohr-Coulomb plasticity analyses. Evaluation of the dam's safety is based on the mode I and II crack analysis and the previous dam safety investigation (Seddon *et al*. 1998).

The dam is loaded by self-weight, hydrostatic pressure at full supply level (FSL), silt pressure, overflow of up to 20 m, uplift pressure, tailwater pressure and a seasonal temperature drop in the dam wall. This loading condition is shown in Figure 7.3. When overflow load is applied, a trapezoidal pressure distribution is acting on the upstream face by adding the FSL triangular pressure with the "overflow" rectangular pressure.

The hydrostatic loadings in the previous dam safety evaluation (Seddon *et al*. 1998) were set for three conditions, as follows:

- Water level at Full Supply Level (FSL - 36.3 m above the rock foundation).
- Water level at Recommended Design Flood (RDF - 4.61 m above the FSL).
- Water level at Safety Evaluation Flood (SEF - 9.99 m above the FSL).

The silt pressure is due to heavy siltation occurring in the dam reservoir which is assumed to be 9 m below the FSL. The density of the silt for the calculation of horizontal silt pressure acting on the upstream face of the dam is 3.53 kN/m$^3$ (Seddon *et al*. 1998).

The uplift pressure has been taken assuming the water level to be at FSL. For overflow conditions such as RDF and SEF, the same uplift pressure is adopted as for FSL, for the reason that higher pressure would not normally have time to develop due to the short duration of flash floods in South Africa.

The elevation of the tailwater is varied with the water level in the dam. When the water level is at FSL, the elevation of the tailwater is at 5.7 m above the foundation. When the water level is at RDF, the elevation of the tailwater is at 15.7 m above the foundation.

When the water level is at SEF, the elevation of the tailwater is at 25.7 m above the foundation.

Concrete dams are also subject to loading by seasonal changes in temperature. Normally, a temperature decrease inside a dam would cause tensile stresses at the upstream heel. Thus a drop in temperature is a loading scenario that must be included in the analysis regarding the safety of a concrete dam.

The drop in temperature for seasonal temperature fluctuations is determined from the standard formula (adopted in the DWAF, South Africa) used in previous arch dam analyses undertaken for South African climatic conditions. This is done due to the lack of more detailed information and the lack of a standard formula for gravity dams.

$$\Delta T = \frac{34}{2{,}4 + t} \tag{7.2}$$

Where t is the thickness (m) of the dam wall at a given level and $\Delta T$ is the temperature drop in degrees Celsius. The temperature distribution was assumed to be uniform through the horizontal section of the dam.

In fact, temperature drop loading makes cracking in this dam propagate even more when compared with the results of load cases without the influence of temperature.

### 7.5.1 Parametric study on the fracture energy of concrete and rock

The fracture energy $G_f$ of the concrete used in dams was discussed and past investigations into it were presented in Section 2.6 of Chapter II. The fracture energy $G_f$ of dam concrete can be set between 100 N/m and 300 N/m. In the present analysis of the dam, a sensitivity study on the concrete fracture energy $G_f^c$ =100 ~ 300 N/m and the rock fracture energy $G_f^r$ =200 ~ 400 N/m is carried out. Different combinations of the fracture energies of concrete and rock based on the above ranges are used in the crack analysis of

this dam. The other fracture parameters used for this sensitivity study are assumed to be as follows:

Bilinear shape parameters $\alpha_1$ = 0.4 and $\alpha_2$ = 0.05; crack onset threshold angle = 30°; maximum shear retention factor $\beta_{\max}$ = 0.1; and tensile strengths for concrete and rock = 1.5 and 2.5 MPa respectively.

Nine graphs of crest horizontal displacement in terms of overflow water level are shown in Figure 7.6. The fracture energy of rock $G_f^r$ appears to have little influence on the crack response of the dam. As the fracture energy of rock increases from 200 N/m to 400 N/m with different values of the fracture energy of concrete $G_f^c$, the structural behaviours become nearly identical for the same fracture energy of concrete $G_f^c$. At low overflow water level, the lower fracture energy of concrete $G_f^c$ (100 N/m) has a higher crest deformation. As the overflow water level increases to a higher level (approximately 17 m above), the crest deformation for a higher fracture energy of concrete $G_f^c$ (300 N/m) becomes larger and increases at a faster rate.

It appears that the fracture energy of concrete and rock in general do not have much influence on the overall dam deformation. The fracture energy of concrete $G_f^c$, however, has a significant influence on the crack propagation paths in the dam structure, as shown in Figures 7.7 to 7.10. All these crack profiles are obtained at the same overflow water level of 20 m. As the fracture energy of concrete $G_f^c$ increases, the crack will propagate from horizontal direction along the concrete/rock interface to bend more into the rock foundation. The fracture energies of concrete $G_f^c$ = 300 N/m and rock $G_f^r$ = 200 ~ 400 N/m will cause the highest deformation in the dam.

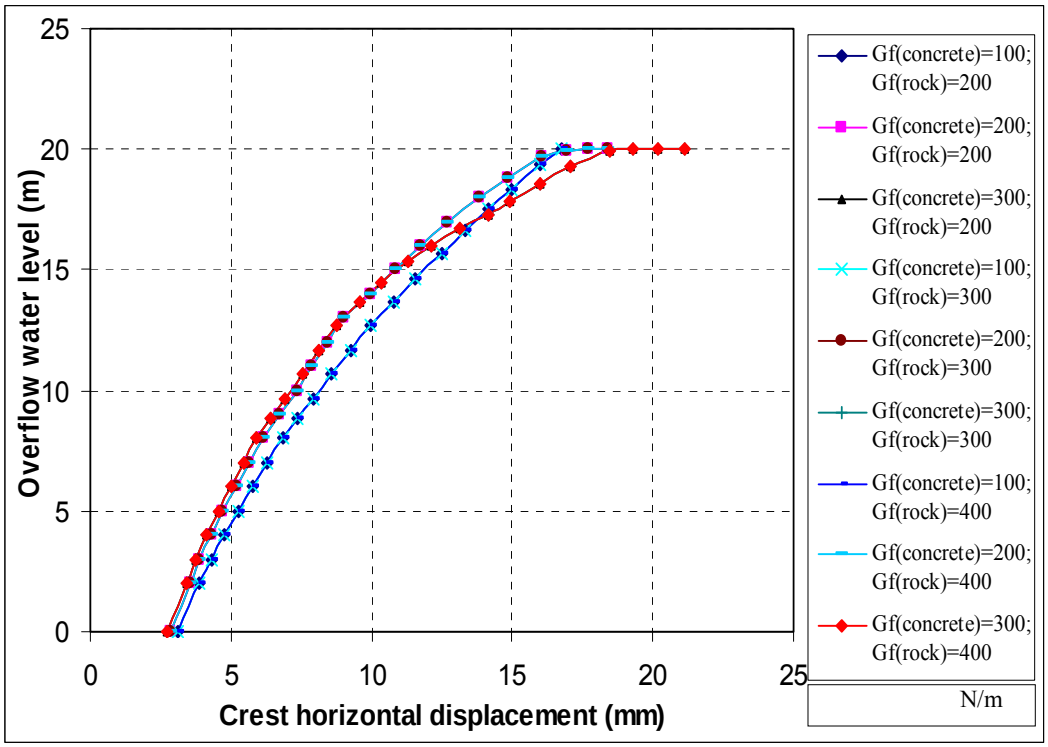


Figure 7.6 - Crest horizontal displacement vs. overflow for various values of fracture energy

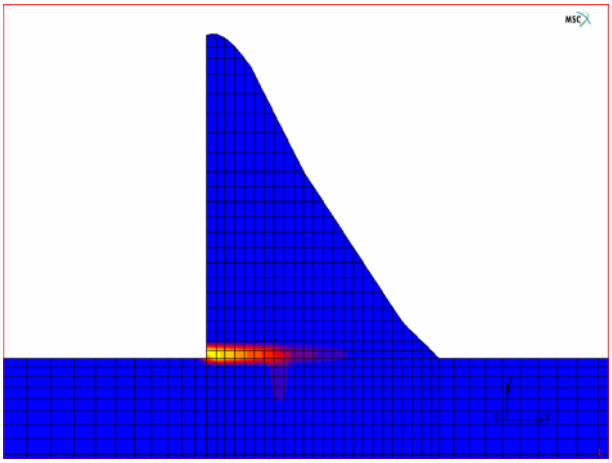

Figure 7.7 - Crack profile for $G_f^c$ = 100 N/m and $G_f^r$ = 400 N/m

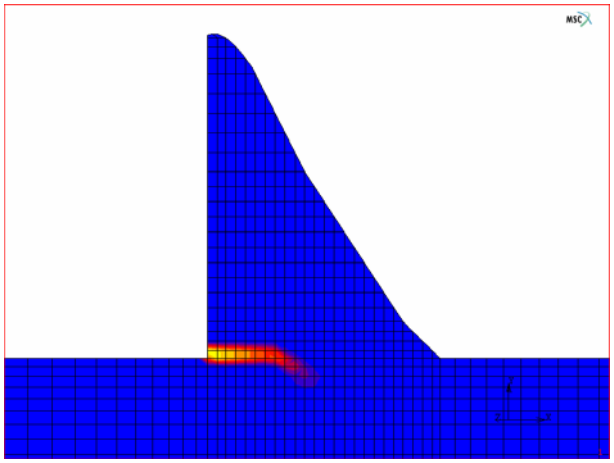

Figure 7.8 - Crack profile for $G_f^c$ = 200 N/m and $G_f^r$ = 400 N/m

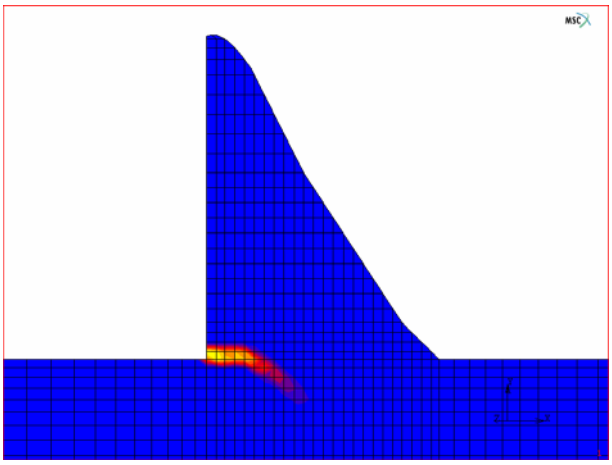

Figure 7.9 - Crack profile for $G_f^c$ =300 N/m and $G_f^r$ = 400 N/m

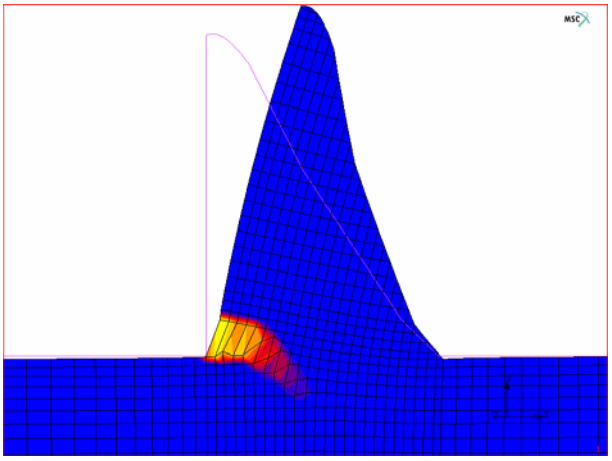

Figure 7.10 - Crack profile for $G_f^c$ = 300 N/m and $G_f^r$ = 400 N/m (deformed shape)

### 7.5.2 Parametric study on the bilinear shape parameters $\alpha_1$ and $\alpha_2$

In accordance with the discussion in Section 7.4 of the concrete used in the dam, the bilinear shape parameters $\alpha_1$ and $\alpha_2$ are studied for their influence on the dam's behaviour. The bilinear shape parameters $\alpha_1$ and $\alpha_2$ for the rock are assumed to be the same as those for the concrete. As stated previously, $\alpha_1$ will be in the range of 0.25 ~ 0.4 and $\alpha_2$ will be 0.05 ~ 0.3. The bilinear mode I strain-softening shapes for different values of $\alpha_1$ and $\alpha_2$ are shown in Figures 7.11 to 7.13.

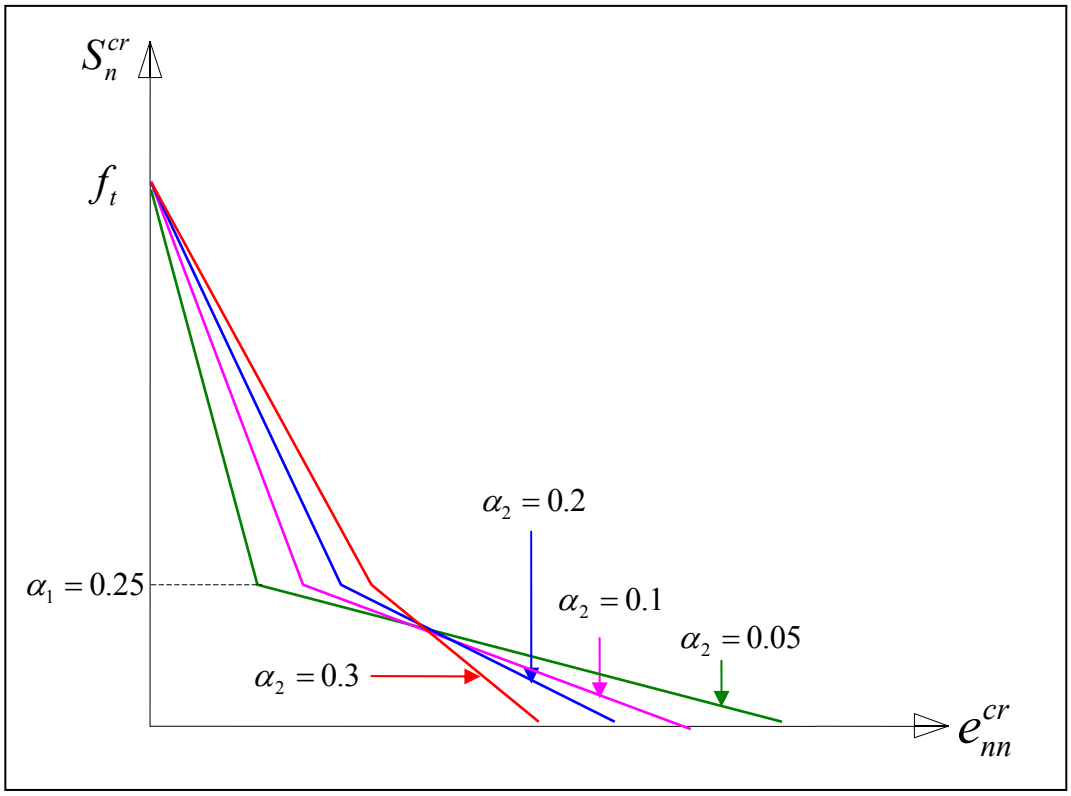


Figure 7.11 - Bilinear softening shapes with $\alpha_1 = 0.25$ and $\alpha_2 = 0.05$, 0.1, 0.2 and 0.3

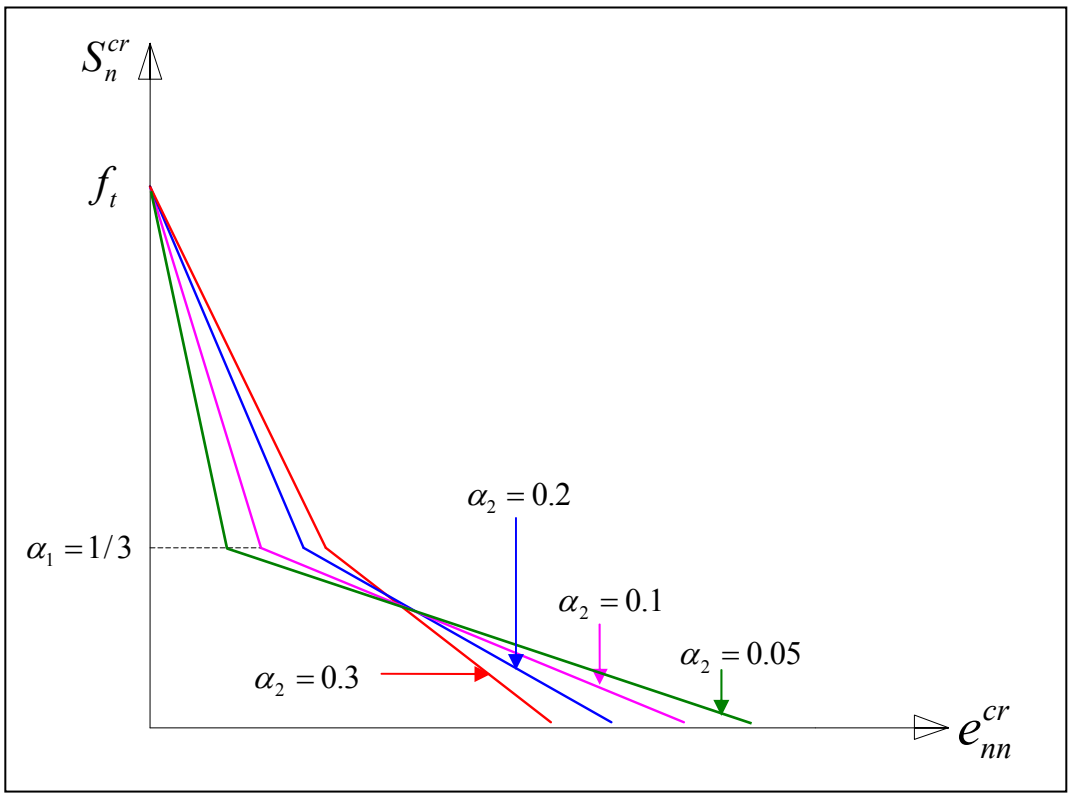


Figure 7.12 - Bilinear softening shapes with $\alpha_1 = 1/3$ and $\alpha_2 = 0.05$, 0.1, 0.2 and 0.3

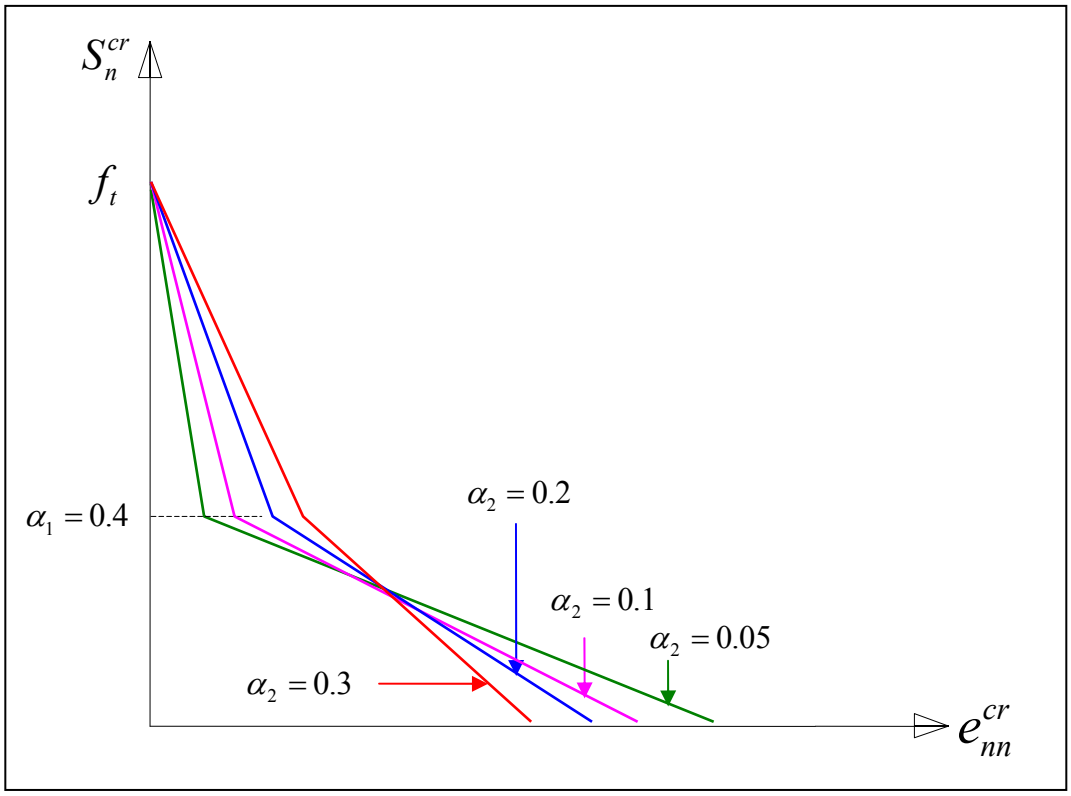


Figure 7.13 - Bilinear softening shapes with $\alpha_1 = 0.4$ and $\alpha_2 = 0.05$, 0.1, 0.2 and 0.3

The other fracture parameters used for this sensitivity study are assumed to be as follows:

Fracture energy $G_f^c$ = 300 N/m and $G_f^r$ = 400 N/m; threshold angle = 30°; maximum shear retention factor $\beta_{\max}$ = 0.1; and tensile strengths for concrete and rock = 1.5 and 2.5 MPa respectively.

As shown in Figures 7.14a to 7.14c, at the low overflow level, the crest deformation for all the combinations of $\alpha_1$ and $\alpha_2$ are similar. When the overflow water level exceeds approximately 7 m, the crest deformation curves of the cases $\alpha_1$ = 1/3; $\alpha_2$ = 0.05 and $\alpha_1$ = 0.4; $\alpha_2$ = 0.05 show significantly more deformation. The other combinations of $\alpha_1$ and $\alpha_2$ have similar crest deformations. The crack profiles (at the same overflow level) shown in Figures 7.15 to 7.26 for different values of $\alpha_1$ and $\alpha_2$ are much more sensitive than the crest deformation. Basically, when $\alpha_1$ is fixed at 0.25 while $\alpha_2$ ranges from 0.05 to 0.3 (see Figures 7.15 to 7.18), cracks in the dam propagate along the concrete/rock interface.

When $\alpha_1$ increases to 1/3 and 0.4 with $\alpha_2$ = 0.05, the crack will propagate by bending downward into the rock (see Figures 7.19 and 7.23). Analyses adopting $\alpha_1$ = 1/3 ~ 0.4 and $\alpha_2$ = 0.05 would cause the dam to deform more.

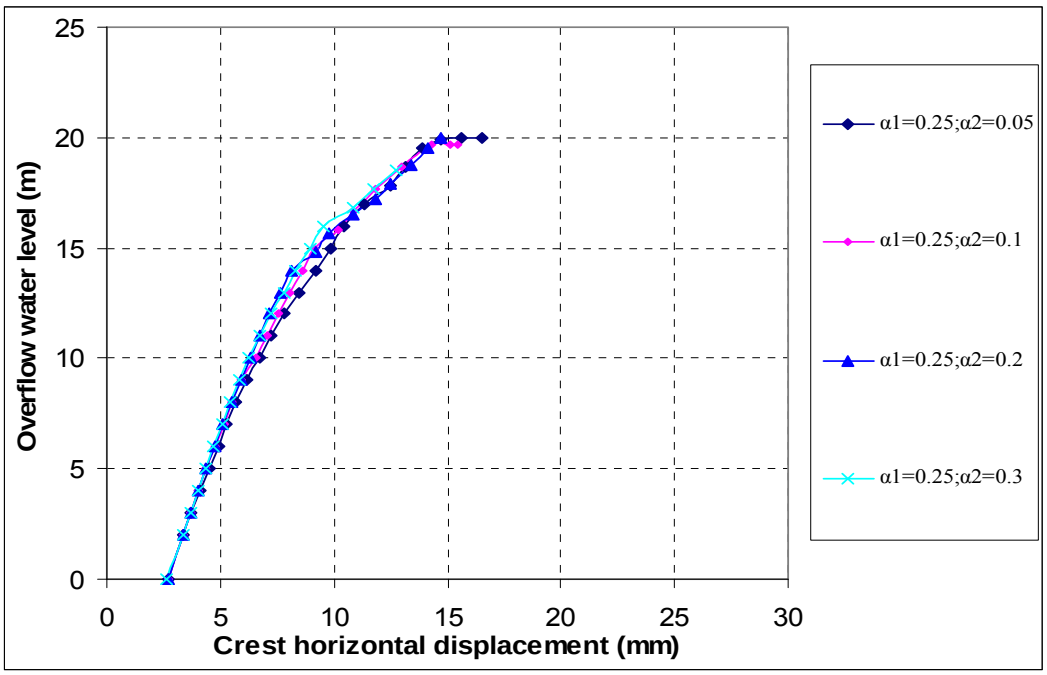


Figure 7.14a - Crest horizontal displacement vs. overflow level for strain-softening relationships with $\alpha_1$ = 0.25 and $\alpha_2$ = 0.05, 0.1, 0.2 and 0.3

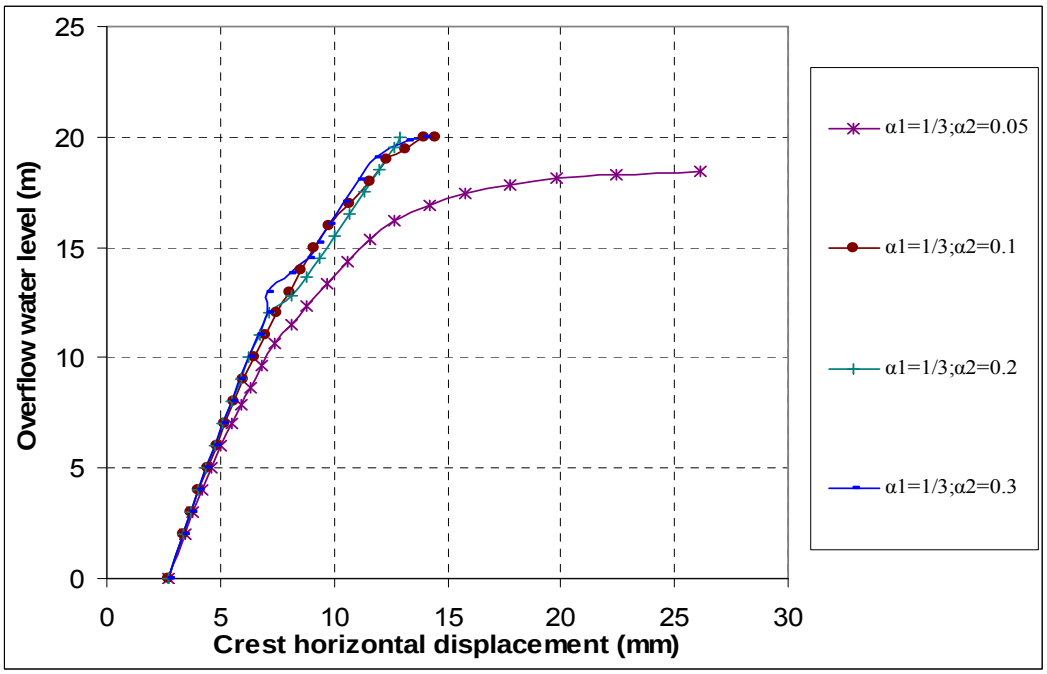


Figure 7.14b - Crest horizontal displacement vs. overflow level for strain-softening relationships with $\alpha_1$ = 1/3 and $\alpha_2$ = 0.05, 0.1, 0.2 and 0.3

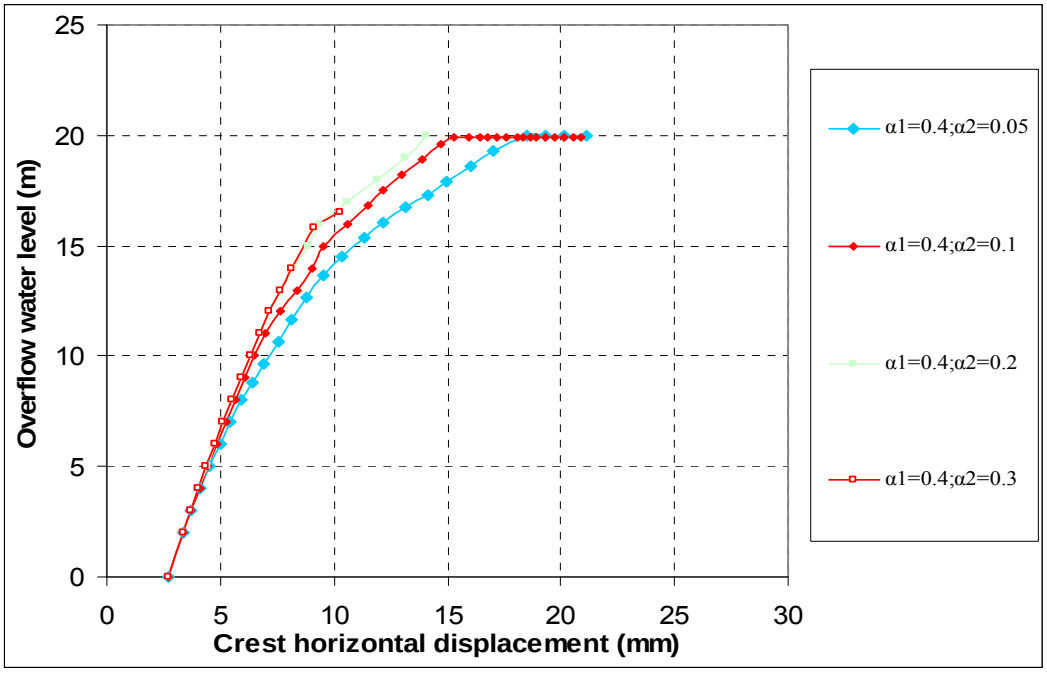


Figure 7.14c - Crest horizontal displacement vs. overflow level for strain-softening relationships with $\alpha_1 = 0.4$ and $\alpha_2 = 0.05$, 0.1, 0.2 and 0.3

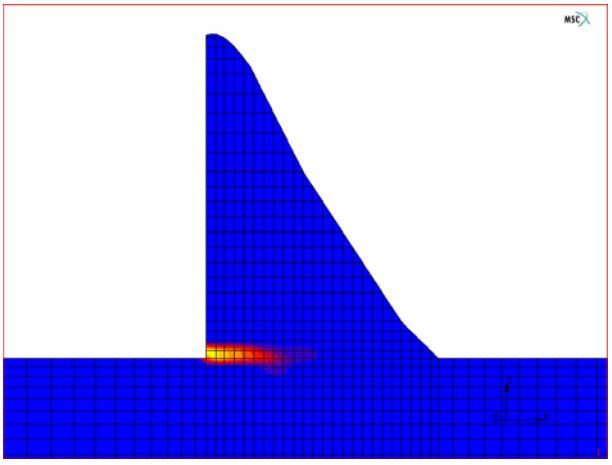

Figure 7.15 - Crack profile for $\alpha_1 = 0.25$ and $\alpha_2 = 0.05$

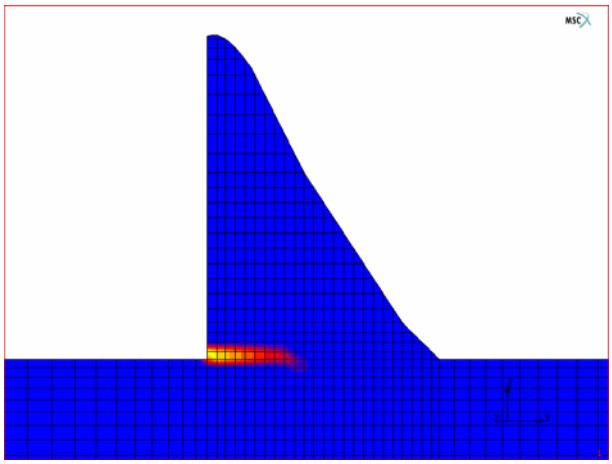

Figure 7.16 - Crack profile for $\alpha_1 = 0.25$ and $\alpha_2 = 0.1$

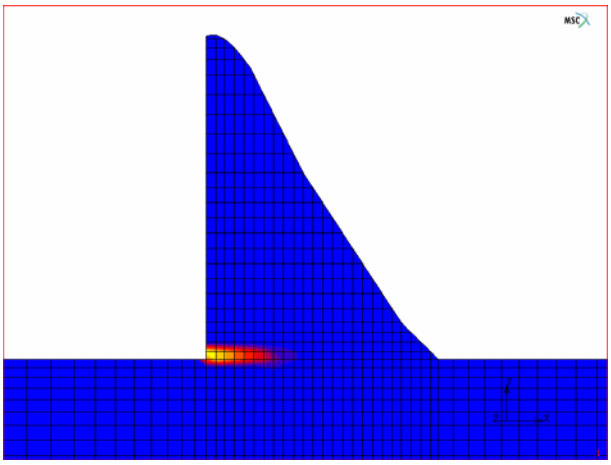

Figure 7.17 - Crack profile for $\alpha_1 = 0.25$ and $\alpha_2 = 0.2$

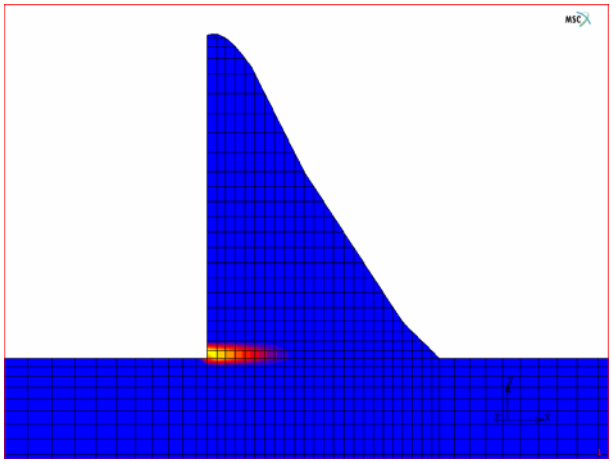

Figure 7.18 - Crack profile for $\alpha_1 = 0.25$ and $\alpha_2 = 0.3$

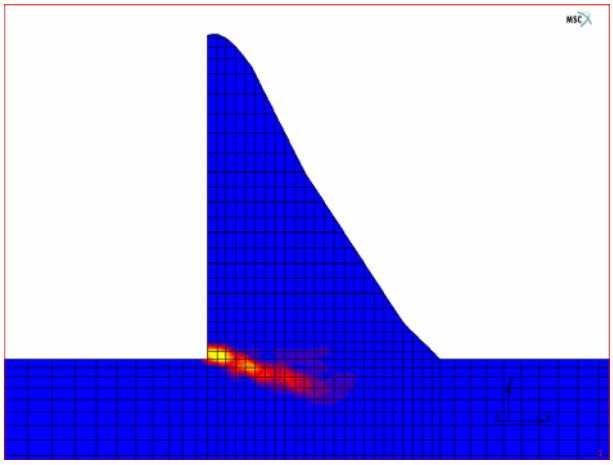

Figure 7.19 - Crack profile for $\alpha_1 = 1/3$ and $\alpha_2 = 0.05$

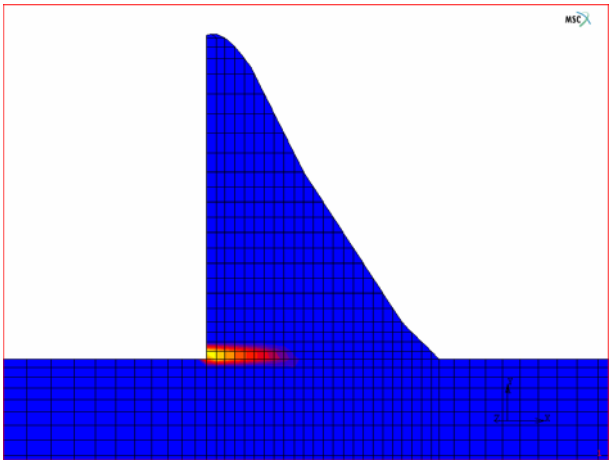

Figure 7.20 - Crack profile for $\alpha_1 = 1/3$ and $\alpha_2 = 0.1$

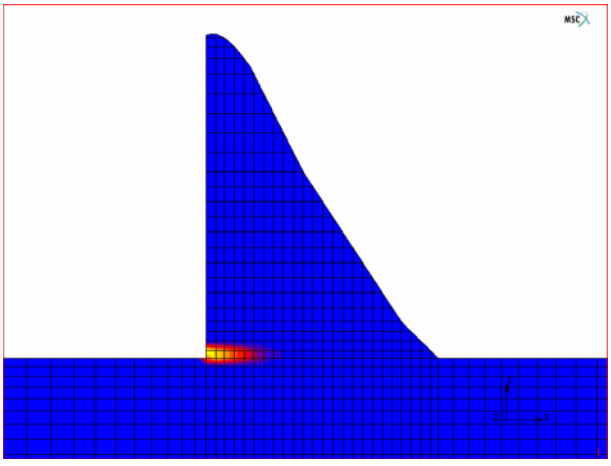

Figure 7.21 - Crack profile for $\alpha_1 = 1/3$ and $\alpha_2 = 0.2$

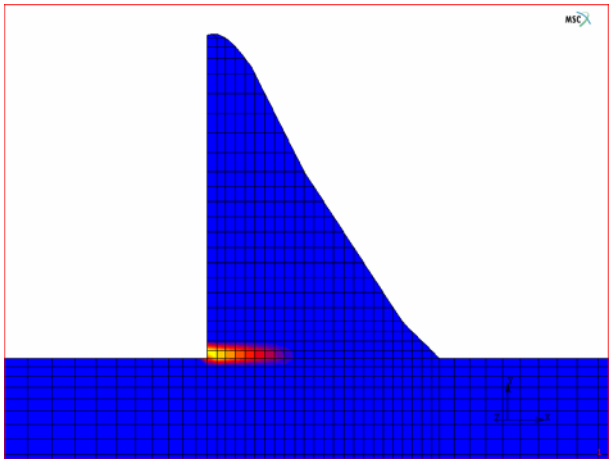

Figure 7.22 - Crack profile for $\alpha_1 = 1/3$ and $\alpha_2 = 0.3$

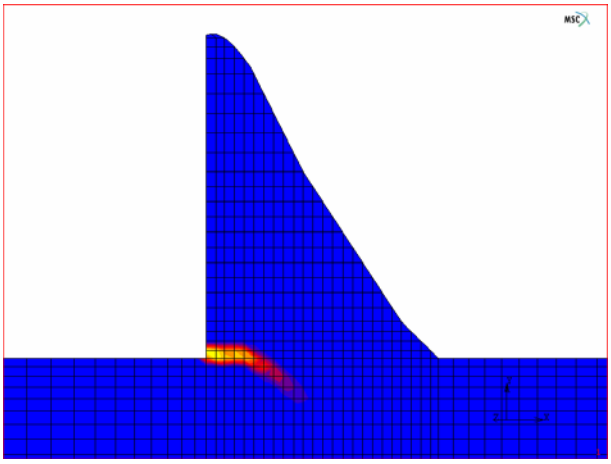

Figure 7.23 - Crack profile for $\alpha_1 = 0.4$ and $\alpha_2 = 0.05$

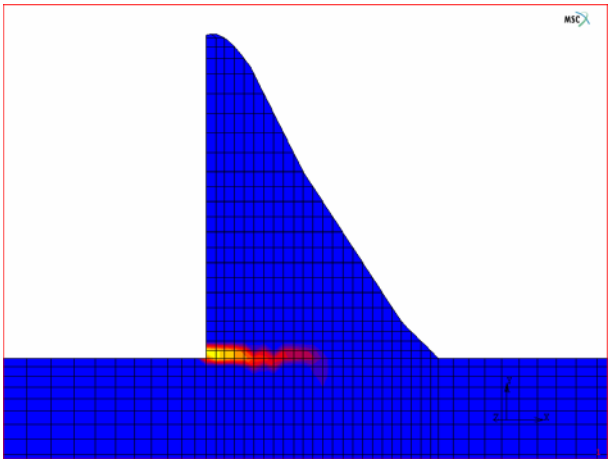

Figure 7.24 - Crack profile for $\alpha_1 = 0.4$ and $\alpha_2 = 0.1$

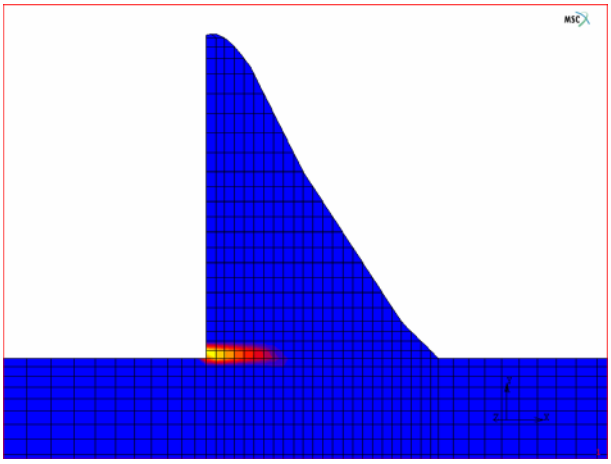

Figure 7.25 - Crack profile for $\alpha_1 = 0.4$ and $\alpha_2 = 0.2$

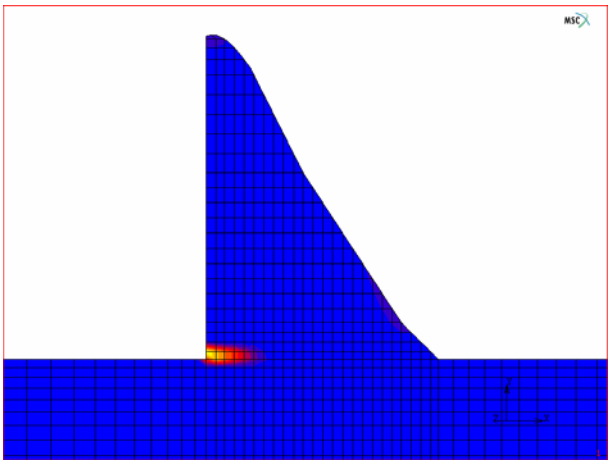

Figure 7.26 - Crack profile for $\alpha_1 = 0.4$ and $\alpha_2 = 0.3$

### 7.5.3 Parametric study on the tensile strength of concrete and rock

The tensile strengths of the wall concrete and the foundation rock for the crack onset criterion are varied to study their influence on the dam behaviour.

The tests on the drilled cores of the dam concrete revealed that the tensile strength of the concrete was 3.07 MPa and the tensile strength of the concrete for analysis can be taken as 1.5 MPa (Van der Spuy 1992). The influence of the tensile strength of the concrete on the crack response of the dam is studied by fixing the tensile strength of the rock $f_t^r$ at

2.5 MPa, while the tensile strength of the concrete $f_t^c$ ranges from 0.002 to 1.5 MPa. The other fracture parameters used for this sensitivity study are assumed to be as follows:

Bilinear shape parameters $\alpha_1$ = 0.4 and $\alpha_2$ = 0.05; threshold angle = 30°; maximum shear retention factor $\beta_{max}$ = 0.1; and fracture energies for concrete and rock = 300 N/m and 400 N/m respectively.

If $f_t^c$ is set equal 0.002 MPa (which represents no tensile strength at the concrete/rock interface as assumed by Seddon *et al*. 1998), the dam would crack through and fail even before water reached the FSL. Thus, the case of $f_t^c$ = 0.002 MPa could not be shown in Figure 7.27. As seen in Figure 7.27, with an increase in the value of $f_t^c$, the dam has less deformation. Therefore, the crack response of the dam is obviously sensitive to the tensile strength of the concrete.

From Figures 7.28 to 7.31 it can be seen that with a higher value of $f_t^c$ for the concrete, the cracks would bend more into the rock.

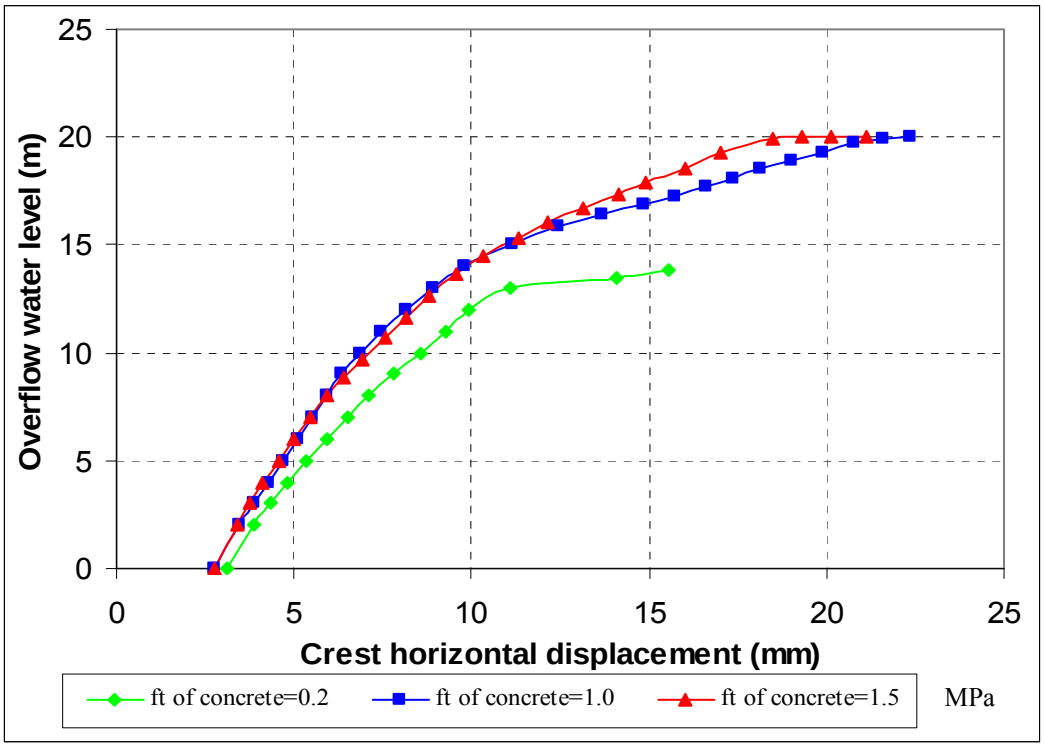


Figure 7.27 - Crest horizontal displacement vs. overflow level for various values of concrete tensile strength

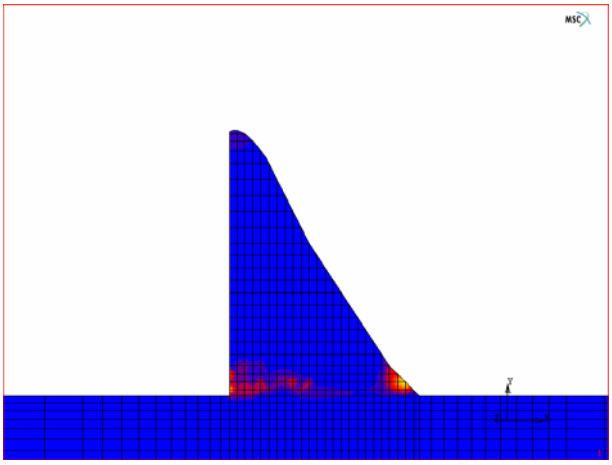

Figure 7.28 - Crack profile for $f_t^c$ = 0.002 MPa and $f_t^r$ = 2.5 MPa

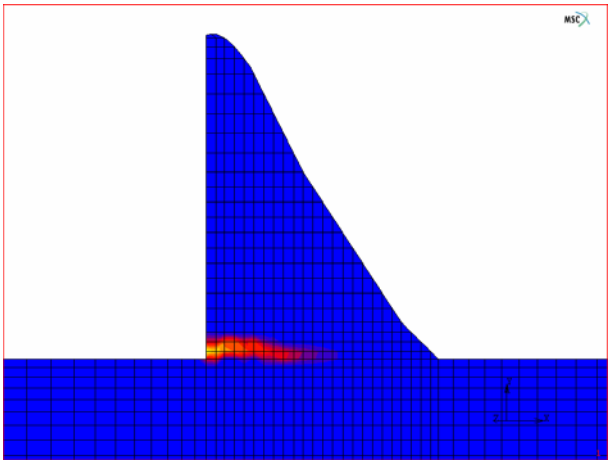

Figure 7.29 - Crack profile for $f_t^c$ = 0.2 MPa and $f_t^r$ = 2.5 MPa

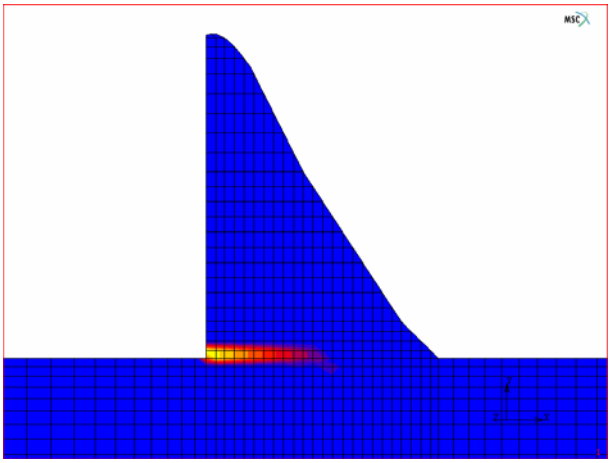

Figure 7.30 - Crack profile for $f_t^c$ = 1.0 MPa and $f_t^r$ = 2.5 MPa

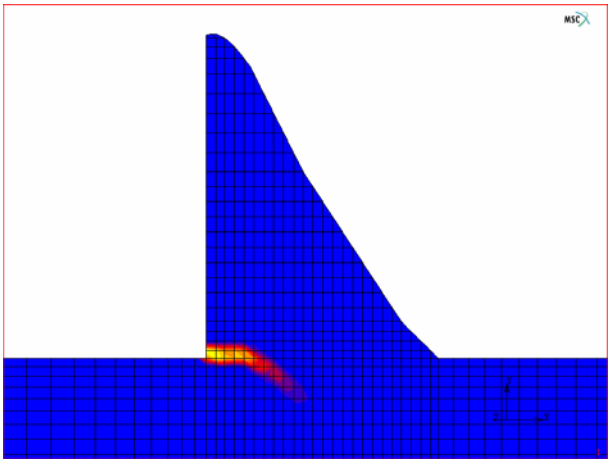

Figure 7.31- Crack profile for $f_t^c$ = 1.5 MPa and $f_t^r$ = 2.5 MPa

### 7.5.4 Parametric study on the crack onset threshold angle $\phi$

Different threshold angles (ranging from 0.1° to 60°) for the crack onset criterion are studied. The threshold angle is discussed in Section 3.6 of Chapter III. The other fracture parameters used for this sensitivity study are assumed to be as follows:

Bilinear shape parameters $\alpha_1$ = 0.4 and $\alpha_2$ = 0.05; fracture energy of concrete and rock = 300 N/m and 400 N/m respectively; maximum shear retention factor $\beta_{\max}$ = 0.1; and tensile strengths for concrete and rock = 1.5 and 2.5 MPa respectively.

From Figure 7.32 it can be seen that there is no clear picture of the influence of the threshold angle on the crest displacement. The crack profiles for the same overflow level of 20 m shown in Figures 7.33 to 7.37 are very sensitive to the threshold angle. The cracks propagate in different directions (bifurcation) in the rock, which probably explains why the crest deformation is not sensitive to the values of the threshold angle.

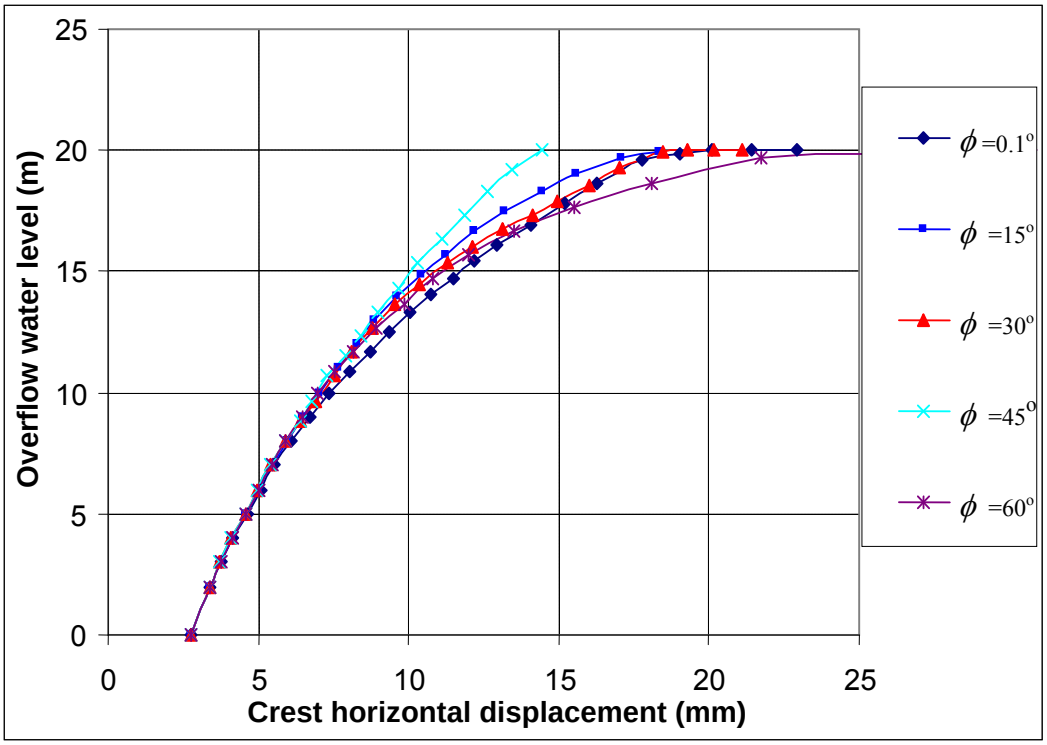


Figure 7.32 - Crest horizontal displacement vs. overflow level for various threshold angles

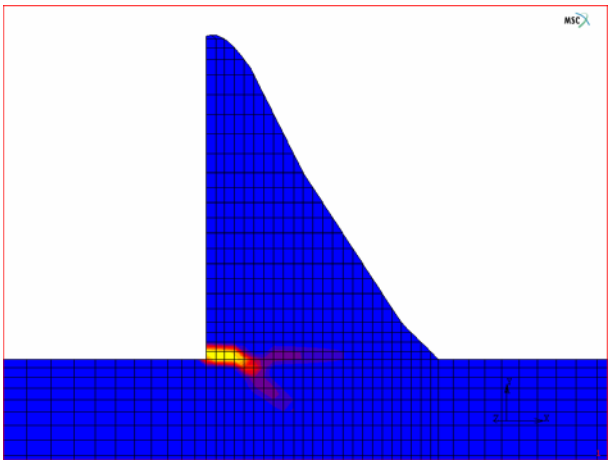

Figure 7.33 - Crack profile for threshold angle of 0.1°

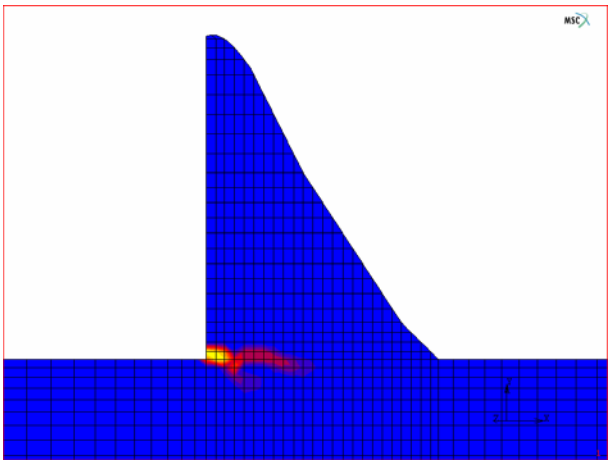

Figure 7.34 - Crack profile for threshold angle of 15°

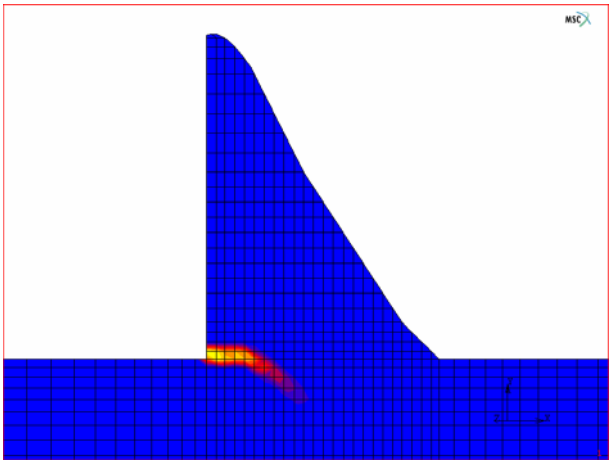

Figure 7.35 - Crack profile for threshold angle of 30$^{o}$

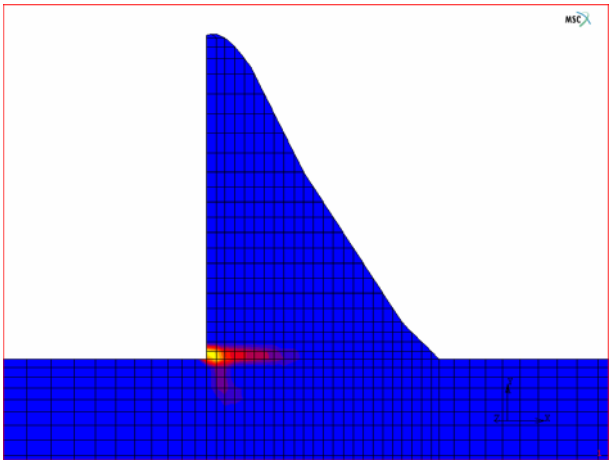

Figure 7.36 - Crack profile for threshold angle of 45$^{o}$

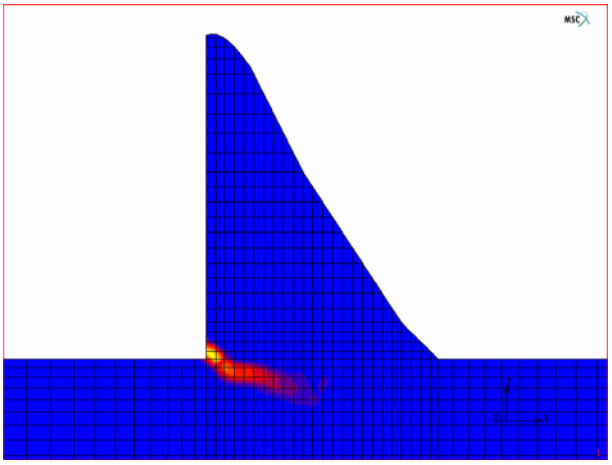

Figure 7.37 - Crack profile for threshold angle of 60$^{o}$

### 7.5.5 Parametric study on the maximum shear retention factor

The influence of the value of the maximum shear retention factor $\beta_{max}$ on the structural behaviour of the dam are studied. The maximum shear retention factor is discussed in Section 3.5 of Chapter III. The other fracture parameters used for this sensitivity study are assumed to be as follows:

Bilinear shape parameters $\alpha_1$ = 0.4 and $\alpha_2$ = 0.05; threshold angle = 30$^{o}$; fracture energy of concrete and rock = 300 N/m and 400 N/m respectively; and tensile strengths for concrete and rock = 1.5 and 2.5 MPa respectively.

Figure 7.38 shows that with a decrease of $\beta_{max}$, the crest deformation becomes larger when the overflow level exceeds approximately 17 m. For higher values of $\beta_{max}$ (0.2 and 0.3), the fracture analysis did not converge beyond overflow levels of 9 m and 15.7 m respectively. Figures 7.39 to 7.42 show that the smaller $\beta_{max}$ is, the sooner and deeper the cracks kink into the rock.

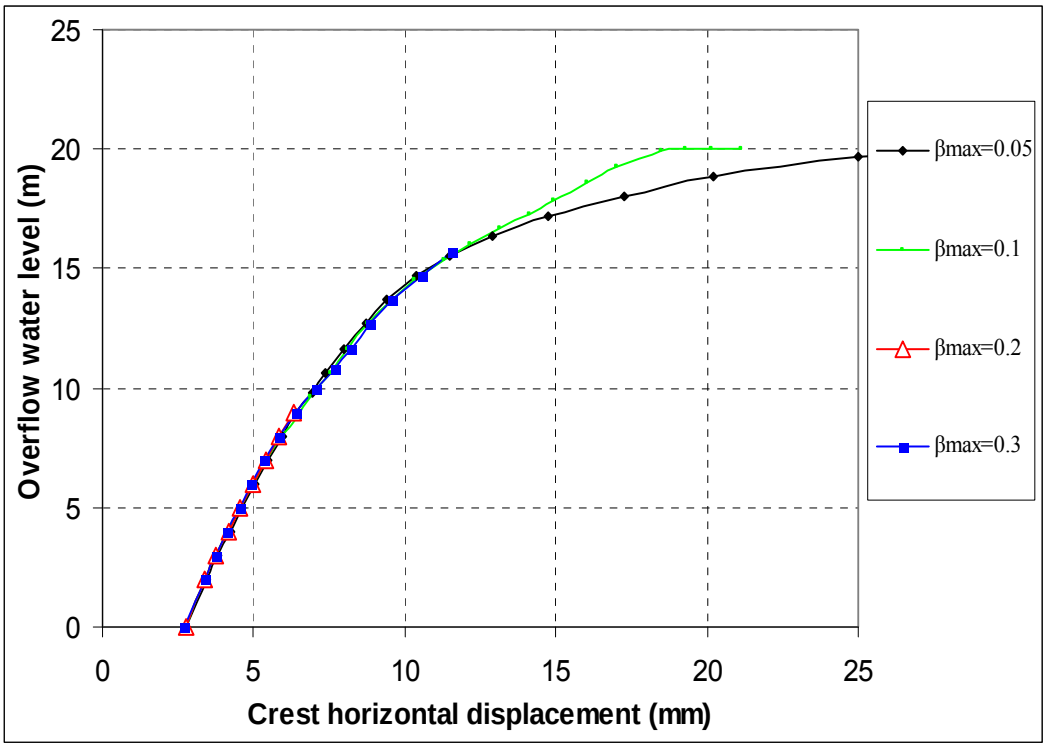


Figure 7.38 - Crest horizontal displacement vs. overflow level for various maximum shear retention factors

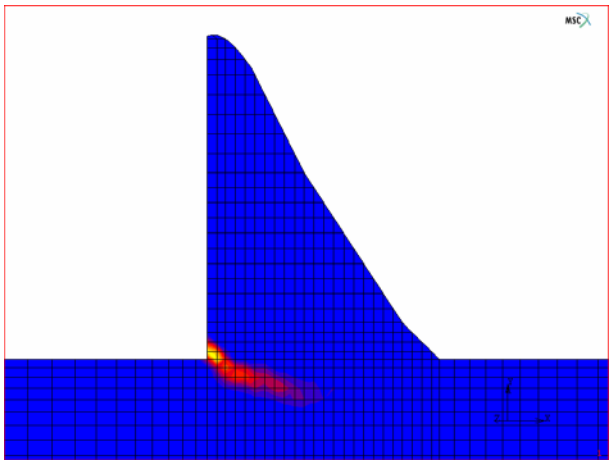

Figure 7.39 - Crack profile for $\beta_{max} = 0.05$

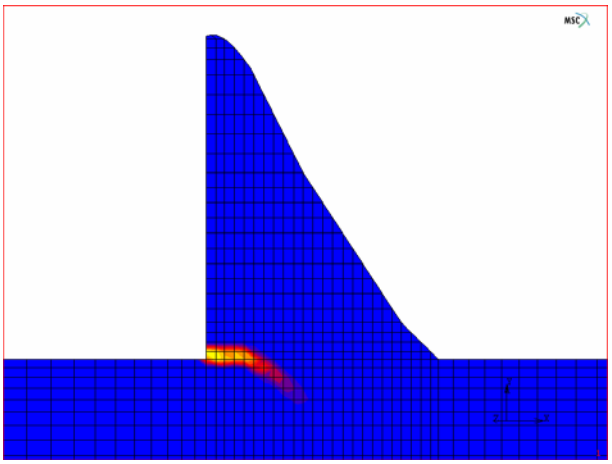

Figure 7.40 - Crack profile for $\beta_{max} = 0.1$

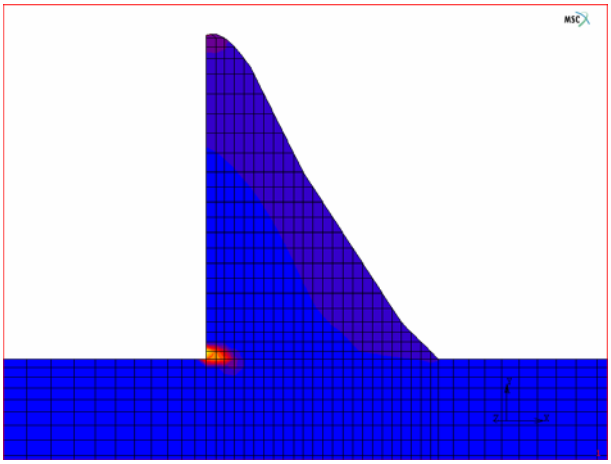

Figure 7.41 - Crack profile for $\beta_{max} = 0.2$

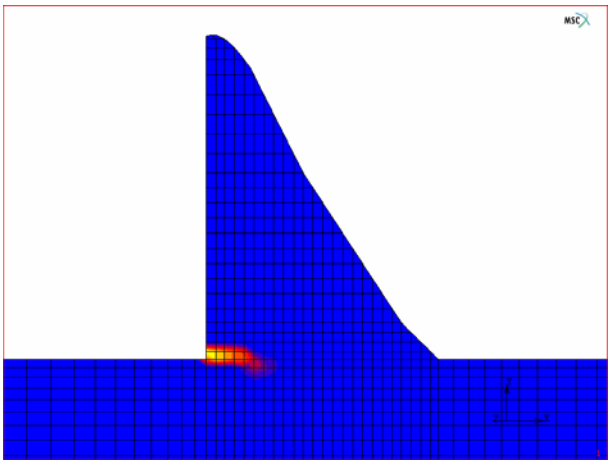

Figure 7.42 - Crack profile for $\beta_{max} = 0.3$

### 7.5.6 Comparison with linear elastic and plasticity analyses

A linear elastic analysis and a non-linear plasticity analysis based on the linear Mohr-Coulomb model are carried out and are compared with the results of various crack analyses. Figures 7.43a to 7.43c show a collection of previous graphs, as well as the results from the linear elastic and plasticity analyses. These graphs are representative of the previous sensitivity studies on fracture parameters. The Mohr-Coulomb yield criteria (refer to Chen & Saleeb 1982) require the cohesion C and the angle of friction $\varphi$ of materials which are provided in Table 7.1.

In some study cases (such as case of $G_f^c$ =100 N/m and $G_f^r$ = 400 N/m) shown in Figure 7.43a, the cracking can be started as early as at FSL while in other cases, the dam starts to crack only after the water level is above FSL.

As can be seen in Figures 7.43a to 7.43c, for fracture analysis of the dam, the crest displacement starts to increase rapidly with an increase in the overflow water level above approximately 17 m over FSL. It appears that the dam is safe at RDF and SEF and can be regarded as unsafe when the overflow water level reaches approximately 17 m.

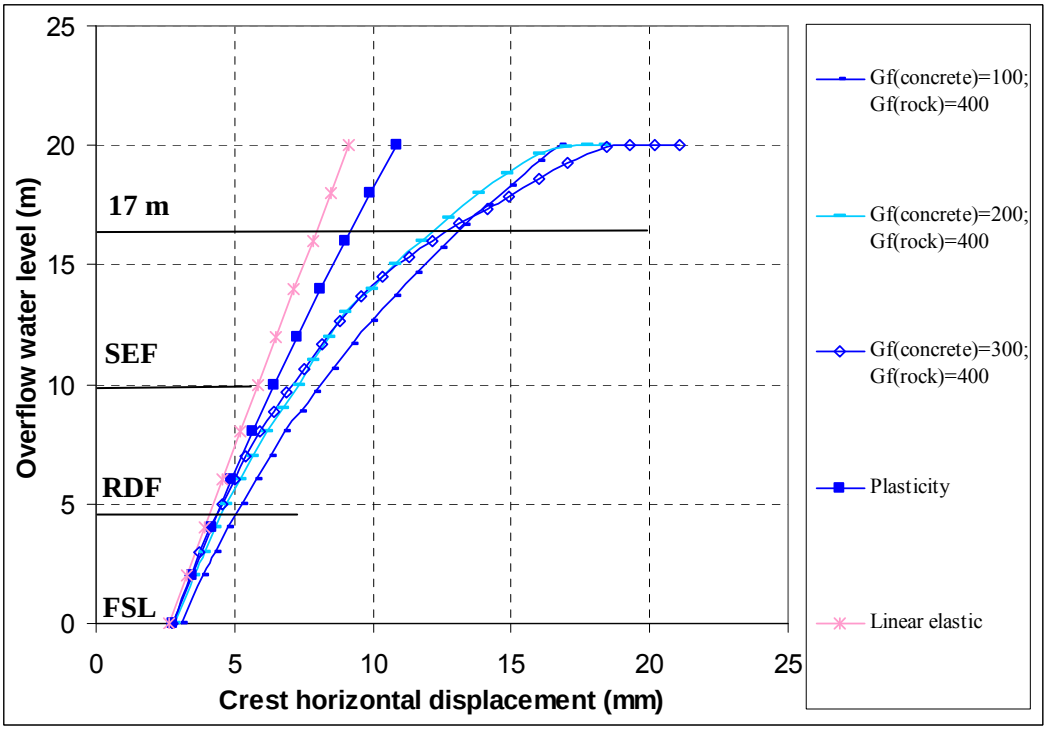


Figure 7.43a - Crest horizontal displacement vs. overflow level for various analysis methods

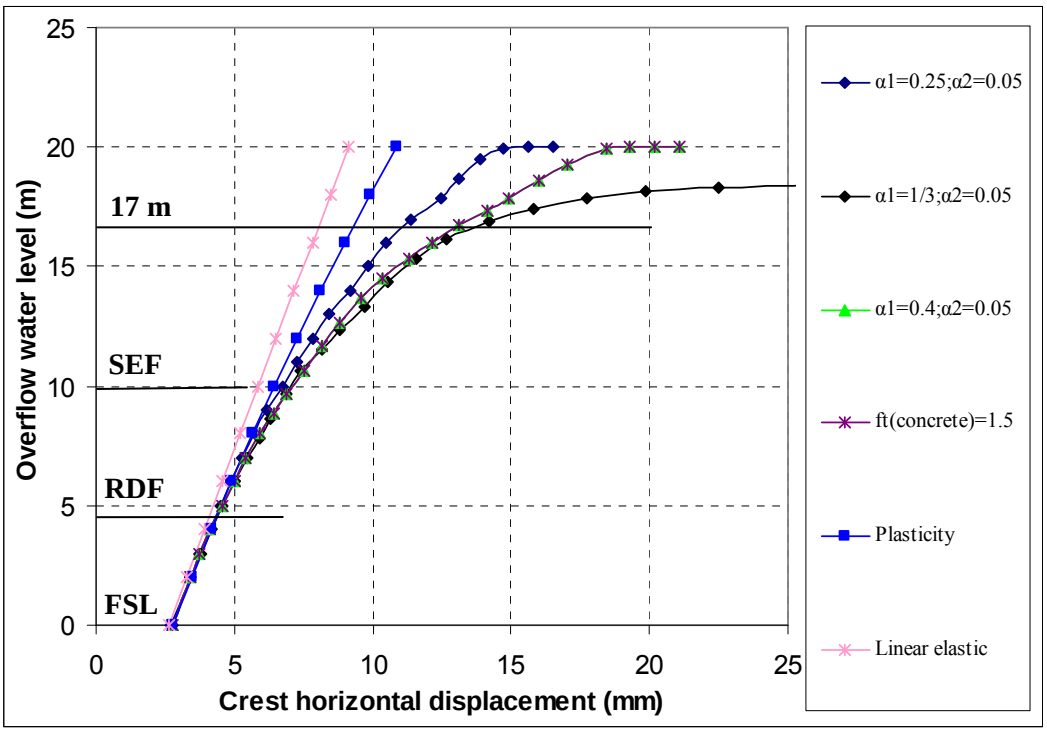


Figure 7.43b - Crest horizontal displacement vs. overflow level for various analysis methods

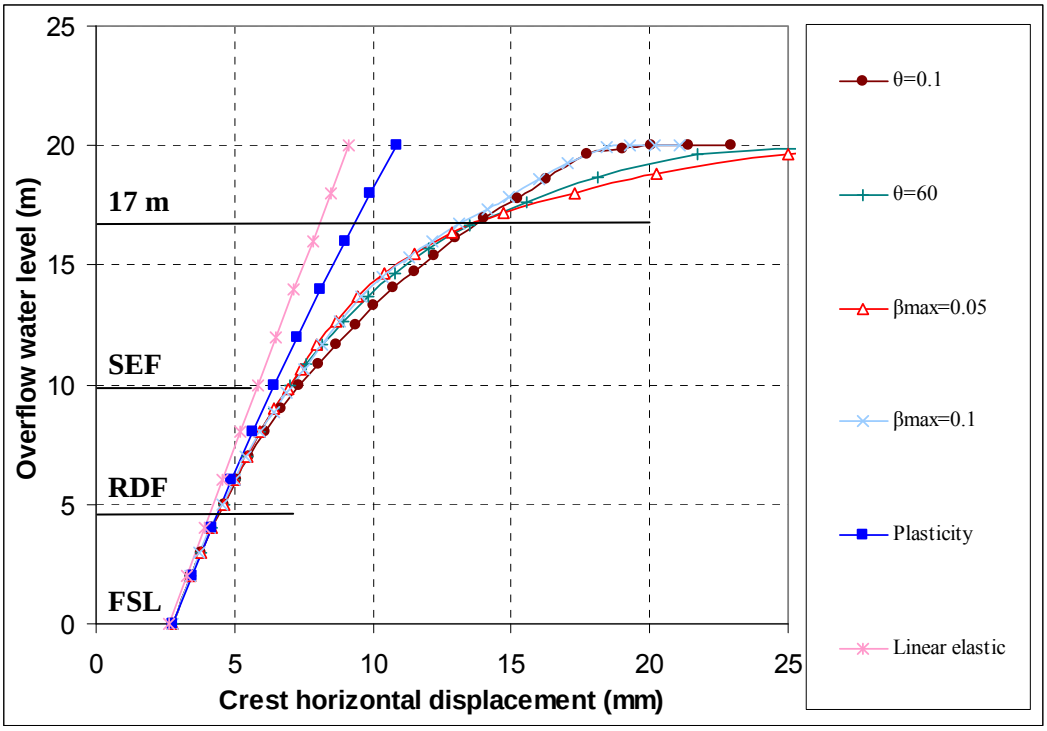


Figure 7.43c - Crest horizontal displacement vs. overflow level for various analysis methods

Subsequently, a new crack analysis is carried out based on the previous sensitivity studies on the fracture parameters (refer to Sections 7.5.1 to 7.5.5). The dam is loaded up to an overflow of 17 m, then unloaded. The constitutive fracture parameters used in this analysis are as follows:

Fracture energy $G_f^c$ = 300 N/m and $G_f^r$ = 400 N/m; bilinear shape parameters $\alpha_1$ = 0.4 and $\alpha_2$ = 0.05; threshold angle = 30°; maximum shear retention factor $\beta_{max}$ = 0.05; and tensile strengths for concrete and rock = 1.5 and 2.5 MPa respectively.

The results are presented in Figures 7.44 to 7.46. Figure 7.44 clearly shows that the dam would crack continuously even under the unloading process (by reducing the overflow water level in the dam). The crest displacement continues to increase with unloading. It is clear that the cracking of the dam is in an unstable stage when the dam is loaded to an overflow of 17 m. Further loading, unloading and even keeping the same loading would make the cracking continue until reaching un-convergence in the analysis. This means that although the local elements may have "failed" due to cracking, the structure as a whole

would still be able to bear some further loading before it failed. This analysis further demonstrates that the dam can be regarded as unsafe when the overflow water level reaches approximately 17 m.

The crack profiles in the dam at the end of loading and unloading are shown in Figures 7.45 and 7.46 respectively. It is clear that the crack propagates further when the dam is in the process of unloading.

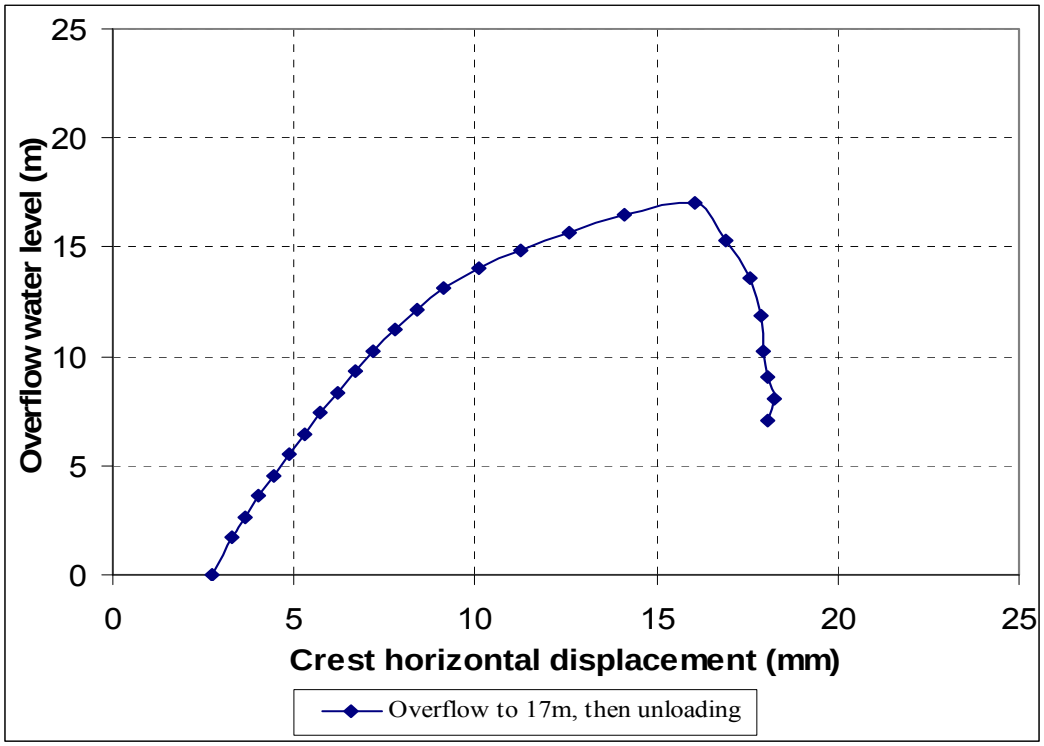


Figure 7.44 - Crest horizontal displacement vs. overflow

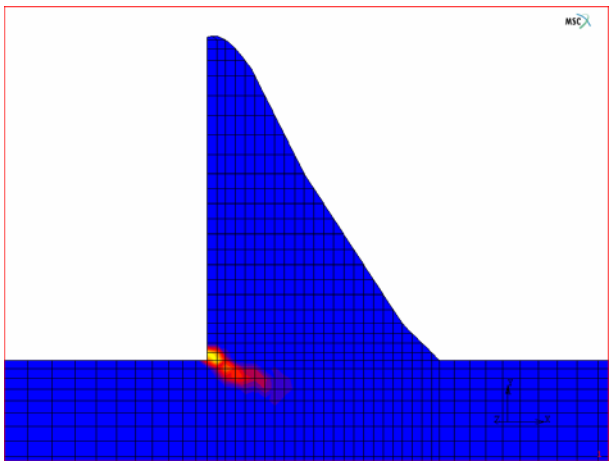

Figure 7.45 - Crack profile for overflow level at 17 m

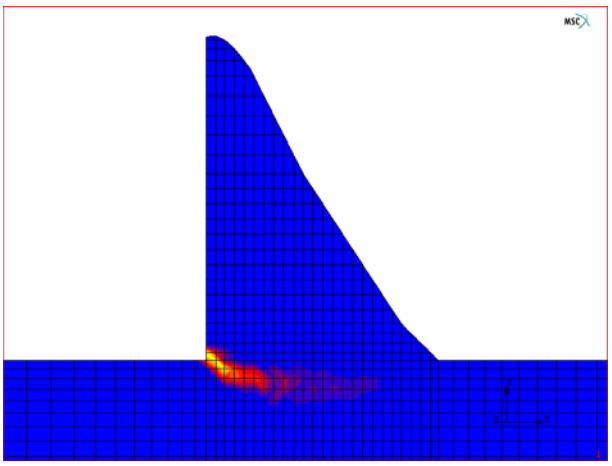

Figure 7.46 - Crack profile at the end of unloading

## 7.6 Evaluation of dam safety against sliding (shear)

As stated in Section 2.2 of Chapter II, the stability of a dam against sliding is of major concern to dam engineers. The classical equation (2.2) for the calculation of the factor of safety against sliding was used to evaluate the safety of this dam (Seddon *et al.,* 1998).

Due to the lack of an alternative method for evaluating the safety of a dam against sliding, in this chapter the horizontal uncracked length along the concrete/rock interface is compared with the calculated critical uncracked length, based on the classical method, to check the stability of the dam against sliding.

The calculated critical uncracked length for the abnormal load cases (20 m overflow, with a factor of safety that should be equal to or greater than 2.0) is 6.12 m, which means that if the uncracked length of the concrete/rock interface is greater than 6.12 m, then the dam is regarded as being safe against sliding (shear) under an overflow water level of 20 m.

Since all the previous sensitivity studies on the fracture parameters have uncracked lengths along the concrete/rock interface longer than the critical uncracked length of 6.12 m, the dam can be regarded as being safe against shear sliding with an overflow water level of up to 20 m.

## 7.7 Conclusions

The safety of the dam was evaluated by Seddon *et al*. (1998) using the traditional gravity method and cracked section analysis (rigid body equilibrium). The findings from their investigation are summarized as follows:

- The dam is stable and failure of the dam is considered very unlikely under FSL (Full Supply Level) condition (no overflow).
- The dam is unstable and the failure of the dam is considered probable under RDF (Recommended Design Flood) condition (overflow 4.6 m)

- The dam is unstable and the failure of the dam is considered possible under SEF (Safety Evaluation Flood) condition (overflow 10 m).

The crack analysis of the dam using the developed non-linear fracture mechanics (NLFM) method reveals that the dam is considered to be safe under FSL, RDF and SEF conditions. The maximum overflow that the dam can endure is found to be at approximately 17 m. Of course, this will leave the dam with no safety margin. Assuming the concrete strength has been taken as the characteristic value, if the overflow at 17 m is taken as a safety factor of 1 (total water level in the dam will be 17 + 36.3 = 53.3 m), then the SEF (9.99 + 36.3 = 46.29 m) will have a safety margin of 53.3/46.29 ≈ **1.15**, the RDF (4.61 + 36.3 = 40.91 m) will have a safety margin of 53.3/40.91 ≈ **1.3** and the FSL (36.3 m) will have a safety margin of 53.3/36.3 ≈ **1.47**.

The NLFM-based investigation into this dam yields a higher collapse load or Imminent Failure Flood (IFF) and provides higher safety factors than those predicted by classical rigid body equilibrium analysis.

The cracking, in general, would start along the concrete/rock interface. Then as the internal shear stresses rise in the rock, the cracking would kink downwards into the rock. This would leave a greater uncracked ligament length along the interface to resist shear sliding, thus giving the dam a higher safety margin.

To cover uncertainties about the material properties and fracture parameters of the concrete and rock, parametric analyses are undertaken for an appropriate structural evaluation concerning the safety of the dam. The influence of the fracture parameters on the cracking response of the dam in terms of crest deformation is summarized as follows:

- The fracture energy $G_f$ normally does not have much influence on the dam's structural behaviour.
- The bilinear shape parameters $\alpha_1$ and $\alpha_2$ produce similar structural responses, except for $\alpha_1$ = 1/3 ~ 0.4 and $\alpha_2$ = 0.05, which would cause more deformation in the dam.

- The tensile strength $f_t^c$ of the concrete has a significant effect on the crack response of the dam. The greater the $f_t^c$, the less crest deformation in the dam and the more cracking into the rock.
- The threshold angle does not have a significant influence on the dam's overall behaviour.
- The maximum shear retention factor $\beta_{max}$ does not have much influence on the dam when the overflow is below approximately 17 m. When the overflow exceeds 17 m, however, the smaller $\beta_{max}$ would cause the dam to deform more.

Nevertheless, the above fracture parameters, in general, do have a big influence on crack growth path, and therefore are sensitive to crack propagation in the dam structure.

It is worth pointing out that if no tensile strength is assumed at the concrete/rock interface, the dam would fail under FSL.

It is also worth pointing out that the water pressure that develops as cracks grow has not been taken into account in this research (or developed NLFM method). Therefore, the findings with regard to the safety of the dam should be taken as the maximum possible (upper boundary) safety limit that the dam can have.